*Journal of Ceramic Processing Research. Vol. 10, No. 6, pp. 705~709 (2009)*

J O U R N A L O F
**Ceramic Processing Research**

# Mechanical alloying and thermal treatment for production of zirconium-iron hydrogen isotope getters

**Kevin M. Fox***
*Savannah River National Laboratory Building 999-W Aiken, SC 29808, USA*

**The objective of this task was to demonstrate that metal hydrides could be produced by mechanical alloying in the quantities needed to support production-scale hydrogen isotope separations. Three starting compositions (ratios of elemental Zr and Fe powders) were selected and attritor milled under argon for times of 8 to 60 hours. In general, milling times of at least 24 hours were required to form the desired $Zr_2Fe$ and $Zr_3Fe$ phases, although a considerable amount of unalloyed Zr and Fe remained. Milling in liquid nitrogen does not appear to provide any advantages over milling in hexane, particularly due to the formation of ZrN after longer milling times. Carbides of Zr formed during some of the milling experiments in hexane. Elemental Zr was present in the as-milled material but not detected after annealing for milling times of 48 and 60 hours. It may be that after intimate mixing of the powders in the attritor mill the annealing temperature was sufficient to allow for the formation of a Zr-Fe alloy. Further investigation of this conversion is necessary, and could provide an opportunity for reducing the amount of unreacted metal powder after milling.**

**Key words: hydrogen absorbing materials, metal hydrides, mechanical alloying; phase transitions, X-ray diffraction.**

## Introduction

Zr-Fe alloys are used as getters for hydrogen and its isotopes. Metal alloy getters are preferred in applications where operation in a nitrogen atmosphere is necessary, and where catalytic oxidation of the isotopes would produce unwanted (and highly toxic) tritiated water. Tritium gettering in Zr-Fe alloys arises through dissolution of atomic tritium in the alloy, which has a low tritium equilibrium partial pressure [1].

A commercially available Zr-Fe alloy, SAES ST198, is often used for hydrogen isotope gettering applications. The chemical composition of ST198 has been reported as 76.5 wt% Zr, 23.5 wt% Fe [2], and 73.6 wt% Zr, 23.3 wt% Fe [3], both of which correspond to $Zr_2Fe$. ST198 has relatively low reactivity with nitrogen [1, 3, 4], making it quite useful for removal of hydrogen isotopes in a nitrogen gas stream. $Zr_2Fe$ has been shown to remain an effective getter material for hydrogen isotopes even as the nitrogen concentration within the alloy becomes significant [5]. However, purification factors decrease as the nitrogen concentration increases, necessitating increased residence times for optimal efficiency [5]. Hydrogen absorption by ST198 is inhibited by $Q_2O$, $CQ_4$ and $NQ_3$ (where Q is any hydrogen isotope) impurities in the gas stream [6]. ST198 also has a high affinity for oxygen, which depletes its gettering capacity for hydrogen isotopes [1]. Typically a ZrMnFe getter, such as the SAES ST909, is used to remove these impurities from the gas stream before it reaches the ST198 getter. ST909 will crack various impurities and retains carbon, nitrogen and oxygen, but very little of the hydrogen isotopes [6].

Several authors have investigated the phases present in ST198 and the stability of these phases after thermal cycling in the presence of hydrogen [3, 4]. ST198 consists mainly of $Zr_2Fe$, with other minor phases including $Zr_5FeSn$, $ZrFe_2$, α-Zr and $Zr_6FeO$ [3]. It is not clear whether the tin-containing phase exists as an impurity or is included intentionally, and difficulty in detecting it via XRD may indicate that it is amorphous [3]. The oxide phase is likely present due to oxygen contamination of the material [3]. $Zr_2Fe$ is considered to be a supercooled or metastable phase, and has been shown to convert to the equilibrium $Zr_3Fe$ phase above 600 °C [3, 4]. Coleman *et al.* provide a summary of crystal structure determinations for $Zr_2Fe$ and $Zr_3Fe$ alloys: $Zr_2Fe$ is body centered tetragonal (*I4/mcm*) and $Zr_3Fe$ is orthorhombic (*Cmcm*) [4]. Hydrides of the $Zr_2Fe$ phase have been shown to be stable at higher temperatures (disproportionation beginning at 400 °C) than those of $Zr_3Fe$ (disproportionation beginning at 200-300 °C) [4]. Hydrides of both phases dissociate upon further heating to $ZrH_x$, α-Fe and $ZrFe_2$ [3, 4].

While the properties and performance of the ST198 material have been well characterized, the method of commercial production is proprietary. Small quantities of the alloy are typically produced for research purposes by arc melting or melt spinning [7, 8], although these techniques are not necessarily economical for production on a large scale. A production method that can produce

*Corresponding author:
Tel : +80-3-819-8462
Fax: +80-3-819-8432
E-mail: kevin.fox@srnl.doe.gov

$Zr_2Fe$ alloys at reasonable cost and in quantities necessary to support hydrogen isotope separations needs is desirable.

## Mechanical Alloying

Mechanical alloying is the process of cold welding, fracturing and re-welding of powder particles in a high-energy mill [9]. This technique can be used to synthesize a variety of metal alloys, as well as metastable phases, currently of interest for use as catalysts and hydrogen storage materials [9]. Mechanical alloying is uniquely suited for the production of metastable phases since, as it is a solid-state processing technique, the thermodynamic and kinetic limitations imposed on other processing methods do not necessarily apply.

Several different types of mechanical mills can be used for alloying. The choice of mill is dependent largely on the amount of material to be produced. The components of the alloy are added to the mill vessel along with the milling media and, in most cases, a small amount of a lubricant such as stearic acid. The mill is then operated at high-speed for periods of minutes to hours.

## Attrition Milling

The attritor, also referred to as a stirred ball mill [10], is a high speed mill used for rapid particle size reduction. Attritors have been developed for both wet and dry grinding applications, and are available in batch and continuous loading configurations. The attritor uses a stationary vessel charged with grinding media and the material to be milled. The mill charge is agitated by a motor driven shaft with horizontal arms. The shaft is rotated at a fairly high speed, which produces high tip velocities at the ends of the agitator arms. This imparts a large amount of energy directly to the milling media.

Size reduction is achieved by impact and shearing forces as the milling media collide with one another. The motion of the agitator arms produces a region of high media turbulence that is at approximately two thirds of the radius from the central shaft [10]. This results in little wear occurring on the vessels walls. Contamination from the vessel walls is therefore reduced, and thinner walls can be used to promote heat transfer and improve temperature control during the milling operation [10].

The size and composition of the milling media used in an attritor has a major impact on its operation [10]. Media used for attrition milling are typically spherical with a diameter of 3-4 mm. Proper selection of media size depends on the size of the initial feed and the intended final particle size. Larger media must be used to grind larger feed material, but smaller media are more effective at fine grinding. The type of material used for the grinding media depends on several factors. When contamination is a concern, materials that are compatible with the feed should be used for both the milling media and the milling vessel. The media should be denser than the feed to prevent floating in the vessel, and harder than the feed to reduce wear. Higher density milling media can greatly reduce milling times.

Batch-type attritors are utilized for dry grinding, particularly when the feed powders must be milled under a protective atmosphere. Material is charged directly into the top of the vessel, can be sampled at any point during the milling process, and additions can be made to the charge without stopping the mill [10]. The vessel can be charged and sealed in an inert glove box prior to milling, or the entire attritor can be contained within a glove box.

In addition to size reduction, the considerable amount of energy imparted to the feed material by an attritor can be used for mechanical alloying of metal particles. The increase in milling energy is due primarily to an increase in the number of media collisions, as evidenced in experiments involving the stress-induced transformation of partially-stabilized zirconia powders [11].

An important aspect of the study described here was to develop a process that could be used to produce the quantities of materials necessary to satisfy the needs of a hydrogen isotope separations facility. Attritor mills are commercially available with capacities many times larger than that used in the tests that are detailed in this report. Therefore, the processes developed with a research-scale attritor could be scaled-up by using larger mills.

## Mechanical Alloying of Metal Hydrides

A small amount of work is available in the literature concerning the fabrication of Zr-Fe-type alloys by mechanical alloying. Hellstern and Schultz reported on mechanical alloying Fe-Zr materials, showing that milling of the elemental metal powders will produce alloys with amorphous structures [12]. They also noted a transformation of α-Zr to the high pressure ω-Zr phase after milling of a $Fe_{20}Zr_{80}$ material [13]. Biegel *et al*. compared the crystallization behavior of amorphous $Fe_{30}Zr_{70}$ alloys prepared by melt spinning and mechanical alloying [7]. The melt spun material crystallized as α-Zr, ω-Zr and $Zr_2Fe$ at moderate temperatures, which then converted to $Zr_3Fe$ above 400 °C. They report that the mechanically alloyed powder crystallized directly to $Zr_3Fe$ [7], although other phases appear to be present in the X-ray diffraction spectra that they present.

Pilar *et al*. investigated the use of various process control agents (PCA) in controlling the amount of cold welding and fracturing that occurs during the mechanical alloying process for FeNiZrB alloys (of interest for their soft magnetic properties) [14]. Milling was completed in a planetary ball mill under argon atmosphere. The results showed that powders milled with hexane and naphthalene formed a more disordered structure with very small crystallite sizes (4 nm) as compared to other organics and powders milled without a PCA. The powders milled in hexane and naphthalene also had better thermal stability after annealing at 450 °C and reduced amounts of oxygen contamination as compared to the other organics, although a significant amount of carbon (> 1.8 at%) remained in the milled powder.

Based on these previous studies, mechanical alloying appears to be a possible route for the fabrication of Zr-Fe alloys for use as getter materials. Heat treatment will likely be necessary to evolve the desired phases after the milling process is completed. The literature provides no clear direction as to the optimum starting composition (ratio of elemental Zr and Fe powders) or the optimum milling conditions. These variables were therefore investigated as part of this study.

## Experimental Procedure

Mechanical alloying experiments were carried out in a large argon glove box facility containing a research-scale attritor mill, an annealing furnace and various powder handling equipment. This allowed all aspects of the mechanical alloying work to be performed under a protective argon atmosphere. Samples were removed only for composition and particle size characterization.

Elemental Zr and Fe metal powders were used as the starting materials for these experiments. Both powders had an initial particle size of -325 mesh and a purity of better than 99%. The attritor mill vessel and agitator were stainless steel. Cylindrical, through-hardened carbon steel (SAE 1065) milling media with convex, hemispherical ends were used. The mill was operated at 650 RPM with chilled kerosene (< 0 °C) cooling.

Three starting compositions were used in these experiments due to the uncertainty in the optimum stoichiometry for application to hydrogen gettering. The elemental Zr and Fe metal powders were added to the mill in mass ratios corresponding to $Zr_2Fe$, $Zr_{2.5}Fe$ and $Zr_3Fe$. Stearic acid was added at 1 wt% as a lubricant. The milled powder was sampled after milling for 8, 24, 48 and 60 hours. The samples were collected and stored under argon. In addition, a milling run with the $Zr_2Fe$ composition was performed with liquid nitrogen ($LN_2$) charged to the milling vessel and sampled at the same intervals. These experiments produced a total of 16 powder samples for characterization.

Upon milling the first composition, $Zr_2Fe$ without $LN_2$, caking of the powder was noted after 8 hours. The powder partially adhered to the grinding media after 24 hours of milling, and completely coated the vessel wall and grinding media after 48 hours of milling. The process was changed to wet grinding with hexane to overcome this problem. The ratio of powder to milling media to hexane was 1 : 5 : 0.5 by volume. After completion of the milling cycle, the hexane was evaporated under vacuum in the oven attached to the glove box, then backfilled with argon for sampling. The powder from the milling run where caking occurred was discarded, and the experiment was re-run using hexane.

Each of the 16 specimens was analyzed by X-ray diffraction (XRD) after milling to identify the crystalline phases present. Loose powder samples of each of the 16 specimens were annealed in argon at 600 °C for 1 hour, since amorphization of the powder was expected after milling. Samples of each of the annealed powders were also analyzed by XRD to determine whether a reduction in amorphization occurred, and if so, to identify the crystalline phases that resulted.

The particle size distribution of each of the milled powder samples (prior to annealing) was measured using a laser light diffraction particle size analyzer.

## Results and Discussion

Each of the milled powder samples was examined by XRD both before and after annealing. A summary of these data is provided in Table 1. After 8 hours of milling, all of the milled powders consisted of unreacted Zr and Fe. Broadening of the XRD peaks was observed for all of the samples, which is indicative of a reduction in average crystallite size. After annealing, the powders milled for 8 hours consisted mainly of unreacted Zr and Fe. ZrC was identified in the $Zr_2Fe$ composition. The $Zr_2Fe$ in $LN_2$ and $Zr_{2.5}Fe$ compositions contained some $Zr_3Fe$, while the $Zr_3Fe$ composition contained some $Zr_4Fe$. A small amount of $Fe_2O_3$ was identified in the $Zr_2Fe$ and $Zr_2Fe$ in $LN_2$ compositions. It is unlikely that this oxygen was picked up from the atmosphere since the partial pressure of oxygen was maintained to a very low value in the glove box. The $Fe_2O_3$ may instead be the result of contamination from the steel attritor mill components and media, which had previously been exposed to air.

All of the starting compositions contained unreacted Zr and Fe after 24 hours of milling. Upon annealing of the powders milled for 24 hours, $Zr_3Fe$ ($Zr_2Fe$ for the powders milled in $LN_2$) crystallized, along with the unreacted Zr and Fe.

After 48 hours of milling, the powders generally remained unreacted Zr and Fe, with the possible inclusion of a small amount of $Zr_4Fe$. Amorphization was apparent in the $Zr_2Fe$ composition milled in $LN_2$ and the $Zr_3Fe$ composition. After annealing, the $Zr_2Fe$, $Zr_{2.5}Fe$ and $Zr_3Fe$ compositions contained $Zr_2Fe$, unreacted Fe, possible $ZrFe_2$ and a series of peaks that were not matched to any phase in the database (labeled 'unidentified phase' in Table 1.). The $Zr_2Fe$ composition milled in $LN_2$ crystallized to mainly ZrN after annealing. Iron-rich Zr-Fe phases and unreacted Fe were also present.

All of the powders milled for 60 hours continued to contain unreacted Zr and Fe. Amorphization of the powders is suggested by the broad hump present in all of the 60 hour XRD spectra. An example XRD spectrum showing this broad hump is given as Fig. 1. An unidentified phase was also present in the $Zr_2Fe$, $Zr_{2.5}Fe$ and $Zr_3Fe$ compositions. After annealing, the $Zr_2Fe$, $Zr_{2.5}Fe$ and $Zr_3Fe$ compositions all contained $Zr_2Fe$, $ZrFe_2$, unreacted Fe and an unidentified phase. The $Zr_2Fe$ composition milled in $LN_2$ again crystallized to mainly ZrN after annealing. Iron-rich Zr-Fe phases and unreacted Fe were also present, as well as an unidentified phase.

**Table 1.** Summary of XRD results for the milled powders

| Composition | Milling Time (h) | Heat Treatment | XRD Results |
|---|---|---|---|
| $Zr_2Fe$ | 8 | as milled | peak broadening, unreacted Zr and Fe |
| | | 600 °C, 1 hour | unreacted Zr and Fe, ZrC, $Fe_2O_3$ |
| | 24 | as milled | largely unreacted Zr and Fe |
| | | 600 °C, 1 hour | $Zr_3Fe$, some unreacted Zr and Fe |
| | 48 | as milled | largely unreacted Zr and Fe, possible $Zr_4Fe$ |
| | | 600 °C, 1 hour | $Zr_2Fe$, unreacted Fe, and unidentified phase |
| | 60 | as milled | amorphization, unreacted Zr and Fe, unidentified phase |
| | | 600 °C, 1 hour | amorphization, $Zr_2Fe$, $ZrFe_2$, unreacted Fe, unidentified phase |
| $Zr_2Fe$ in $LN_2$ | 8 | as milled | peak broadening, unreacted Zr and Fe |
| | | 600 °C, 1 hour | unreacted Zr and Fe, $Zr_3Fe$, possible $Fe_2O_3$ |
| | 24 | as milled | unreacted Zr and Fe, possible $Zr_4Fe$ |
| | | 600 °C, 1 hour | $Zr_2Fe$, unreacted Zr and Fe |
| | 48 | as milled | amorphization, unreacted Zr and Fe, possible $Zr_4Fe$ |
| | | 600 °C, 1 hour | crystallized ZrN, $ZrFe_2$, $Zr_6Fe_{23}$, unreacted Fe |
| | 60 | as milled | amorphization, possible $Zr_3Fe$, unreacted Zr and Fe |
| | | 600 °C, 1 hour | crystallized ZrN, possible $Zr_6Fe_{23}$, unreacted Fe, unidentified phase |
| $Zr_{2.5}Fe$ | 8 | as milled | peak broadening, unreacted Zr and Fe |
| | | 600 °C, 1 hour | unreacted Zr and Fe, $Zr_3Fe$ |
| | 24 | as milled | unreacted Zr and Fe, possible $Zr_4Fe$ |
| | | 600 °C, 1 hour | unreacted Zr and Fe, $Zr_3Fe$, ZrC, $Fe_2O_3$ |
| | 48 | as milled | unreacted Zr and Fe, possible $Zr_4Fe$ |
| | | 600 °C, 1 hour | $Zr_2Fe$, $ZrFe_2$, unreacted Fe, unidentified phase |
| | 60 | as milled | amorphization, unreacted Zr and Fe, unidentified phase |
| | | 600 °C, 1 hour | $Zr_2Fe$, $ZrFe_2$, unreacted Fe, unidentified phase |
| $Zr_3Fe$ | 8 | as milled | peak broadening, unreacted Zr and Fe |
| | | 600 °C, 1 hour | unreacted Zr and Fe, $Zr_4Fe$ |
| | 24 | as milled | unreacted Zr and Fe, possible $Zr_4Fe$ |
| | | 600 °C, 1 hour | $Zr_3Fe$, unreacted Zr and Fe |
| | 48 | as milled | amorphization, $Zr_4Fe$, unreacted Zr and Fe |
| | | 600 °C, 1 hour | $Zr_2Fe$, possible $ZrFe_2$, unreacted Fe, unidentified phase |
| | 60 | as milled | amorphization, unreacted Zr and Fe, unidentified phase |
| | | 600 °C, 1 hour | $Zr_2Fe$, $ZrFe_2$, unreacted Fe, unidentified phase |

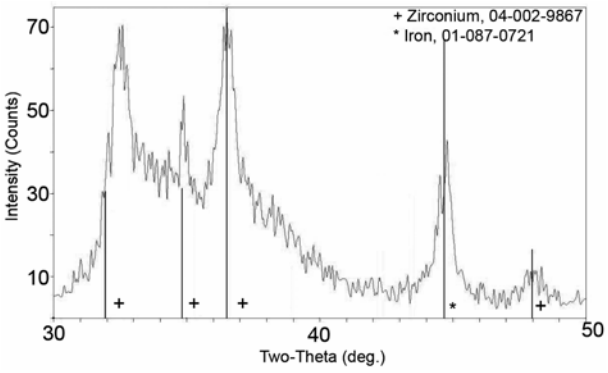


**Fig. 1.** XRD spectrum for the $Zr_3Fe$ sample after milling for 60 hours. Note the broad background hump due to amorphization of the powder. This sample also contains unidentified crystalline peaks.

It is unusual to note that for all the powders milled for 48 or 60 hours, Zr was present in the as-milled material but not detected after annealing. It may be that after intimate mixing of the powders in the attritor mill, the annealing temperature of 600 °C was high enough to allow for the formation of a Zr-Fe alloy. The phase diagram for the binary Zr-Fe system indicates that $Zr_3Fe$ should be stable at the annealing temperature (600 °C) [15]. Further investigation of this conversion is necessary, and could provide an opportunity for reducing the amount of unreacted metal powder after milling. In addition, unreacted Fe remained in all of the powders after annealing for all of the milling times tested. This may indicate that the ratio of Zr to Fe needs to be increased in order to improve the yield of the desired Zr-Fe alloys.

Fig. 2 provides a representative example of the results of the particle size analyses for each of the four milling runs. An analysis was performed at each sampling interval. In general, the results show that as milling time is increased, the particle size distribution becomes broader and shifts to a smaller average size. This is not surprising, as longer milling times provide the time and energy input necessary

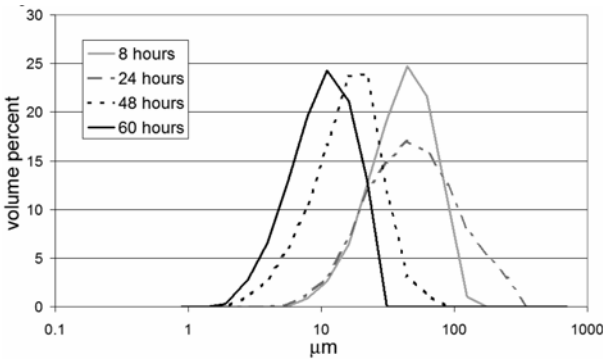


**Fig. 2.** Particle size analysis results for the mechanically alloyed $Zr_2Fe$ mixture sampled at four intervals. Results for the other compositions were similar.

to further fracture the powder particles. No effort was made to de-agglomerate or control the surface chemistry of the powders. Therefore it is likely that these measurements represent the size of agglomerates in the powders, while the actual crystallite size is considerably smaller.

## Conclusions

In general, milling times of at least 24 hours were required to form the desired $Zr_2Fe$ and $Zr_3Fe$ phases, although a considerable amount of unalloyed Zr and Fe remained before annealing. Milling in $LN_2$ does not appear to provide any advantages over milling in hexane, particularly due to the formation of ZrN after longer milling times.

Carbides of Zr formed during some of the milling experiments in hexane. While ZrC was identified in only two of the milled powders, further XRD analysis may show that some of the unidentified peaks belong to carbide phases. Formation of carbides during milling appears to be much less of an issue than formation of nitrides (i.e., a much smaller fraction of the Zr powder appears to form carbides, leaving more Zr for the formation of Zr-Fe alloys). Additional XRD experiments should be designed to improve signal to noise ratio (i.e., longer count times) and use a wider scan range to better identify phases that were not clear in the original data.

Elemental Zr was present in the as-milled material but not detected after annealing for milling times of 48 and 60 hours. It may be that after intimate mixing of the powders in the attritor mill the annealing temperature was sufficient to allow for the formation of a Zr-Fe alloy. The phase diagram for the binary Zr-Fe system agrees with this proposition. If this is the case, then the annealing conditions should also be investigated and optimized to form as much of the Zr-Fe alloy as possible in the milled powder. Also, this finding would mean that milling times of more than 48 hours are not required. Further investigation of this conversion is necessary, and could provide an opportunity for reducing the amount of unreacted metal powder after milling. Elemental Fe remained in all of the powders after annealing for all of the milling times tested. This may indicate that the ratio of Zr to Fe needs to be increased in order to improve the yield of the desired Zr-Fe alloys.

## Acknowledgements

The author would like to acknowledge funding provided by the Department of Energy (DOE) National Nuclear Security Administration (NNSA) Plant Directed Research and Development Program at the Savannah River Site. Initial work on this study was completed by Dr. James Congdon at SRNL. The author extends thanks to Xiaodi (Scott) Huang and the Institute of Materials Processing at Michigan Technological University for skilled assistance with the mechanical alloying work, and Arthur Jurgensen and David Missimer at SRNL for interpretation of the XRD data.

## References

1. J.E. Klein and J.R. Wermer, Fusion Technology, 28[10] 1532-1539 (1995).
2. C. Boffito, F. Doni and L. Rosai, Journal of the Less Common Metals 104[1] 149-157 (1984).
3. A. Nobile, W.C. Mosley, J.S. Holder and K.N. Brooks, U.S. Department of Energy Report WSRC-TR-92-557, Revision 1, Westinghouse Savannah River Company, Aiken, SC (1994).
4. M. Coleman, D. Chandra, J. Wermer and T. Udovic, Advanced Materials for Energy Conversion II, edited by D. Chandra, R. G. Bautista and L. Schlapbach. TMS (The Minerals, Metals & Materials Society), pp. 429-435 (2004).
5. K.J. Maynard, N.P. Kherani and W.T. Shmayda, Fusion Technology, 28[10] 1546-1551 (1995).
6. E.J. Larson, K.J. Cook, J.R. Wermer and D.G. Tuggle, U.S. Department of Energy Report LA-UR-CO-3896, Los Alamos National Laboratory, Los Alamos, NM (2000).
7. W. Biegel, H.U. Krebs, C. Michaelsen and H.C. Freyhardt, Materials Science and Engineering, 97 59-62 (1988).
8. V.A. Yartys, H. Fjellvåg, I.R. Harris, B.C. Hauback, A.B. Riabov, M.H. Sørby and I. Y. Zavaliy, Journal of Alloys and Compounds, 293-295 74-87 (1999).
9. C. Suryananrayana, Materials Science and Engineering, 304-306 151-158 (2001).
10. J.E. Becker, The American Ceramic Society Bulletin, 75[5] 72-74 (1996).
11. M.C. Kerr and J.S. Reed, American Ceramic Society Bulletin, 71[12] 1809-1816 (1992).
12. E. Hellstern and L. Schultz, Materials Science and Engineering, 97 39-42 (1988).
13. E. Hellstern and L. Schultz, Applied Physics Letters, 49[18] 1163-1165 (1986).
14. M. Pilar, J. J. Sunol, J. Bonastre and L. Escoda, Journal of Non-Crystalline Solids, 353 848-850 (2007).
15. T.B. Massalski and H. Okamoto, Binary Alloy Phase Diagrams, ASM International, Materials Park, OH (1990).